fluids

MDPI

Article

The Asymptotic Structure of Canonical Wall-Bounded Turbulent Flows

Stefan Heinz

Department of Mathematics and Statistics, University of Wyoming, 1000 E. University Avenue, Laramie, WY 82071, USA; heinz@uwyo.edu

Abstract: Our ability to reliably and efficiently predict complex high-Reynolds-number (*Re*) turbulent flows is essential for dealing with a large variety of problems of practical relevance. However, experiments as well as computational methods such as direct numerical simulation (DNS) and large eddy simulation (LES) face serious questions regarding their applicability to high *Re* turbulent flows. The most promising option to create reliable guidelines for experimental and computational studies is the use of analytical conclusions. An essential criterion for the reliability of such analytical conclusions is the inclusion of a physically plausible explanation of the asymptotic turbulence regime at infinite *Re* in consistency with observed physical requirements. Corresponding analytical results are reported here for three canonical wall-bounded turbulent flows: channel flow, pipe flow, and the zero-pressure gradient turbulent boundary layer. The asymptotic structure of the mean velocity and characteristic turbulence velocity, length, and time scales is analytically determined. In outer scaling, a stable asymptotic mean velocity distribution is found corresponding to a linear probability density function of mean velocities along the wall-normal direction, which is modified through wake effects. Turbulence tends to decay in this regime. In inner scaling, the mean velocity is governed by a universal log-law. Turbulence does survive in an infinitesimally thin layer very close to the wall.

Keywords: wall-bounded turbulent flows; infinite Reynolds number; mean flow structure; turbulence structure

Citation: Heinz, S. The Asymptotic Structure of Canonical Wall-Bounded Turbulent Flows. *Fluids* **2024**, *9*, 25. https://doi.org/10.3390/fluids9010025

Academic Editors: Nilanjan Chakraborty and Martin Skote

Received: 1 December 2023
Revised: 4 January 2024
Accepted: 10 January 2024
Published: 17 January 2024

1. Introduction

The understanding of the structure of wall-bounded turbulent flows has been a vibrant topic of classical fluid mechanics for almost a century [1–14]. The problem that the Reynolds number (*Re*) usually has a strong influence on the flow structure, and our ability to reliably study turbulent flows at very high *Re* using direct numerical simulation (DNS) or experiments is rather limited [15]. Of specific interest and relevance is the asymptotic structure of wall-bounded turbulent flows at infinite *Re*, and the *Re* scaling of how a potentially existing asymptotic state is reached. Such knowledge can provide valuable guidelines for DNS and experimental studies, the evaluation of promising new developments as determined through minimal error simulation methods [16–20], the development of improved turbulence models [21], the understanding of scaling regimes [22], and the better understanding of asymptotic structures of other turbulent flows [20]. There exist prior studies on a potential asymptotic state of canonical wall-bounded flows, but such studies face questions. For example, Kollmann used pipe flow models that include modeling assumptions in contradiction to the universality of the law of the wall [23]. Pullin et al. assumed log-law mean velocity variations above a certain distance from the wall and developed wake model assumptions in conjunction with debated log-law type assumptions for streamwise turbulence intensities to derive conclusions about asymptotic turbulence [24].

The motivation for this paper is to address the question about the potential existence of an asymptotic state of canonical wall-bounded turbulent flows on the basis of recent modeling of the mean flow and Reynolds shear stress for channel flow, pipe flow, and the zero-pressure gradient turbulent boundary layer (TBL) (for simplicity, the zero-pressure gradient TBL will be referred to simply as TBL) [6,7]. The latter models were obtained through thorough analyses of the physics of these flows up to the highest available Re. The model considered is presented next, followed by analyses of outer and inner scaling consequences. Conclusions are presented in the last section.

2. The Probabilistic Velocity Model

An analytical model for the mean velocity U^+ and Reynolds shear stress $-\langle u'v'\rangle^+$ introduced by Heinz [6,7] for turbulent channel flow, pipe flow, and the TBL is described in Table 1. In particular, the Reynolds shear stress $-\langle u'v'\rangle^+$ for the three flows considered is determined via the momentum balance $S^+ - \langle u'v'\rangle^+ = M$ used in conjunction with models for the total stress M; see Table 1. The momentum balance also involves the characteristic shear rate $S^+ = \partial U^+/\partial y^+$. The superscript + refers to inner scaling; we use $U^+ = U/u_\tau$ and $y^+ = Re_\tau y$ for the inner scaling wall distance, where y is normalized by δ (the half-channel height, pipe radius, or 99% boundary-layer thickness with respect to channel flow, pipe flow, and the TBL). The friction Reynolds number is defined by $Re_\tau = u_\tau \delta/\nu$, where u_τ is the friction velocity and ν is the constant kinematic viscosity.

Table 1. The analytical PVM model valid for $Re_\tau \geq 500$ [6,7]. Here, $B_G()$ refers to the incomplete beta function [25] with subscript G, and $(\cdots,\cdots,\cdots)$ refers to channel flow, pipe flow, and TBL. Corresponding Reynolds shear stress models are given via the momentum balance $S^+ - \langle u'v'\rangle^+ = M$. Here, M refers to the total stress given by $M = (M_{CP}, M_{CP}, M_{BL})$ used in conjunction with $M_{CP} = 1 - y$ and $M_{BL} = e^{-y^6 - 1.57y^2}$.

$$U^+ = U_1^+ + \frac{1}{\kappa}\, ln\left(\frac{1 + Hy^+/y_\kappa}{w + Ky}\right) \qquad \bullet\ H = \left[\frac{y^+/h_1}{1 + y^+/h_1}\right]^{h_3}, \quad K = (0.933, 0.687, 0.285)$$

- $U_1^+ = a\left[cB_G\left(c + \frac{c}{b}, 1 - \frac{c}{b}\right) + G^{\frac{c}{b}}(1-G)^{-\frac{c}{b}} - G^{c+\frac{c}{b}}(1-G)^{-\frac{c}{b}}\right], \quad G = \frac{(y^+/a)^{b/c}}{1 + (y^+/a)^{b/c}}$
- $w = (w_{CP}, w_{CP}, w_{BL}), \quad w_{CP} = 0.1(1-y)^2\left[6y^2 + 11y + 10\right], \quad w_{BL} = e^{-y(0.9 + y + 1.09y^2)}$

$$S^+ = S_1^+ + S_2^+ + S_3^+ + S_1^{CP} + S_2^{CP}$$

- $S_1^+ = 1 - \left[\frac{(y^+/a)^{b/c}}{1 + (y^+/a)^{b/c}}\right]^c, \quad \kappa y^+ S_2^+ = \frac{1 + h_3/[1 + y^+/h_1]}{1 + y_\kappa/(y^+ H)}, \quad \kappa y^+ S_3^+ = -\frac{1 + w'/K}{1 + w/(Ky)}$
- $S_1^{CP} = -yS_1^+(1)\frac{1 - S_1^+}{1 - S_1^+(1)}, \quad S_2^{CP} = -yS_2^+\left(1 - \left[\kappa Re_\tau S_2^+(1)\right]^{-1}\right)$

- $\kappa = 0.40,\ y_\kappa = 75.8,\ a = 9,\ b = 3.04,\ c = 1.4,\ h_1 = 12.36,\ h_3 = 6.47.$

The model for the mean velocity U^+ and Reynolds shear stress $-\langle u'v'\rangle^+$ presented in Table 1 was derived for $Re_\tau \geq 500$. A specific feature of the model is the approach to designing it. First, several observational physics requirements were identified. Via analysis of DNS and experimental data, the model was derived by providing explicit evidence that the model satisfies all observational physics criteria. The latter included evidence that both modeled variables and their relevant derivatives accurately represented the corresponding observations in regard to all the relevant scalings. The model's excellent performance in comparison to DNS [26–30] and experimental data [31–34] for channel flow, pipe flow, and the TBL is described elsewhere [6,7]. These comparisons include a model validation up to $Re_\tau = 98{,}190$, corresponding to $Re \sim 6.3$ M [7]. The velocity model is referred to as the probabilistic velocity model (PVM) because it determines the distribution function for the distribution of mean velocities along the wall-normal direction and its related probability density function (PDF); see the discussion below.

Essential details of the PVM structure are explained in terms of Figure 1. This figure reveals the mode structure of the PVM given by the contributions S_1^+, S_2^+, and S_3^+ to the characteristic shear rate $S^+ = \partial U^+/\partial y^+$. The latter mode contributions are related to corresponding velocity contributions U_1^+, U_2^+, and U_3^+. Here, S_1^+ and S_2^+ (which are only functions of y^+) are inner scaling contributions. For all the three flows considered, S_1^+ and S_2^+ are the same. In contrast to that, $\kappa y^+ S_3^+$ (which is only a function of y) is an outer scaling contribution: it depends on the flow considered. There are also two inner scale correction terms, S_1^{CP} and S_2^{CP} (see Table 1). They have an irrelevant effect on the mean velocity; these contributions only matter in regard to the correct calculation of turbulent viscosities for channel and pipe flow. A relevant conclusion of Figure 1a is that the PVM implies a universal log-law. In particular, the PVM implies $U^+ = \kappa^{-1} ln\, y^+ + 5.03$ for all the three flows considered in absence of boundary effects. This log-law involves a universal von Kármán constant $\kappa = 0.40$ for the three flows considered. As explained in detail elsewhere [7], there are critical Reynolds numbers of Re_τ =20,000, Re_τ =63,000, and Re_τ =80,000 for the observation of a strict log-law for channel flow, pipe flow, and the TBL, respectively.

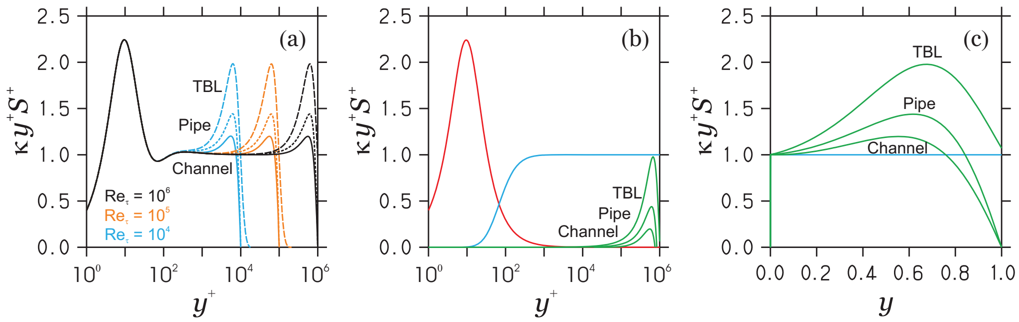

Figure 1. The log-law indicator $\kappa y^+ S^+$ (with $\kappa = 0.4$) obtained from the PVM is shown in (**a**) for the given Re_τ and the three flows considered (channel flow: solid line; pipe flow: short dashes; TBL: long dashes). In (**b**), the mode contributions $\kappa y^+ S_1^+$ (red line), $\kappa y^+ S_2^+$ (cyan line), and $\kappa y^+ S_3^+$ (green lines) are shown for $Re_\tau = 10^6$ in inner scaling. In (**c**), mode contributions $\kappa y^+ S_2^+$ (cyan line) and $\kappa y^+ (S_2^+ + S_3^+)$ (green lines) are shown for $Re_\tau = 10^6$ in outer scaling. There is no visible $\kappa y^+ S_1^+$ mode contribution.

3. Outer Scaling Implications

The outer scaling implications of the PVM are considered first by focusing on variations in y. Apart from considering y variations, this requires the use of the appropriate outer velocity scale U_∞, as opposed to the use of u_τ for inner scaling variations. The difference between U_∞ and u_τ is significant: we have $U_\infty/u_\tau = U_\infty^+ = 5.03 + \kappa^{-1} ln(Re_\tau/K)$. An overview of corresponding scaling variables and their relationships is presented in Table 2. A difference is made in regard to inner and outer scaling and inner-scale and outer-scale variables: inner and outer scaling refers to looking at variations along y^+ and y, respectively, whereas inner-scale and outer-scale variables refer to the normalization of variables using corresponding characteristic velocity and length scales.

Table 2. Overview of inner and outer scaling variables. Here, $U_\infty^+ = 5.03 + \kappa^{-1} ln(Re_\tau/K)$ is the centerline/freestream maximum velocity. $Re_* = \nu_t^+$ is equivalent to the inner-scale turbulence viscosity.

	Outer-Scale Variables	Inner-Scale Variables
Scaling velocity and length	U_∞, δ	u_τ, δ
Reynolds number	$Re = U_\infty \delta/\nu = U_\infty^+ Re_\tau$	$Re_\tau = u_\tau \delta/\nu$
Turbulence velocity scale	$u_\infty = \sqrt{-\langle u'v' \rangle^+}/U_\infty^+ = u_*/U_\infty^+$	$u_* = \sqrt{-\langle u'v' \rangle^+}$
Turbulence time scale	$\tau_\infty = U_\infty^+/(S^+ Re_\tau) = \tau_* U_\infty^+/Re_\tau$	$\tau_* = 1/S^+$
Turbulence length scale	$\ell_\infty = u_\infty \tau_\infty = \ell_*/Re_\tau$	$\ell_* = u_* \tau_* = \sqrt{-\langle u'v' \rangle^+}/S^+$
Turbulence *Re*	$Re_\infty = u_\infty \ell_\infty = Re_*/(U_\infty^+ Re_\tau)$	$Re_* = u_* \ell_* = -\langle u'v' \rangle^+/S^+$

Figure 2 shows the outer scaling variations in the outer-scale velocity U^+/U^+_∞ for the three flows considered. It may be seen that U^+ converges with the constant centerline/freestream maximum velocity U^+_∞, but the convergence is extremely slow. Upon closer inspection, Equation (1) shows that the plateau value in these plots is given by $ln(Re_\tau y)/ln(Re_\tau)$. This means that not only Re_τ has to become sufficiently large, but $ln(Re_\tau)$ needs to be sufficiently large, too. This figure supports the view that a mean velocity equal to U^+_∞ cannot be realized in reality because such Re_τ values cannot be realized.

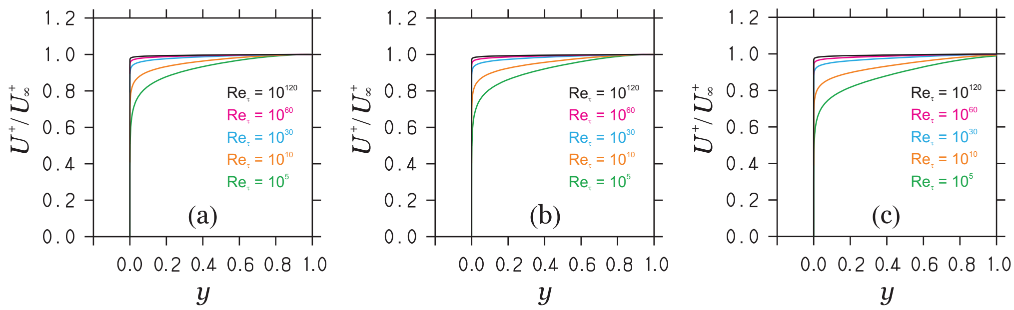

Figure 2. Asymptotic outer velocity scaling with Re_τ along y: (**a**) channel flow, (**b**) pipe flow, (**c**) TBL.

A different picture of the convergence of the velocity distribution can be seen by considering the asymptotic variation of U^+ implied by the PVM, which is given by

$$U^+_{as} = U^+_\infty + \frac{1}{\kappa} ln\Big(\frac{Ky}{Ky+w}\Big) = 5.03 + \frac{1}{\kappa} ln\Big(\frac{Re_\tau}{K}\Big) + \frac{1}{\kappa} ln(Ky) + U^+_3 = \frac{1}{\kappa} ln(y^+) + 5.03 + U^+_3, \tag{1}$$

where the definitions $U^+_\infty = 5.03 + \kappa^{-1} ln(Re_\tau/K)$ and $U^+_3 = -\kappa^{-1} ln(Ky + w)$ are used (U^+_3 is the wake contribution to U^+ based on S^+_3). As shown in Figure 3, U^+ converges to this asymptotic scaling at a much lower Re_τ: at $Re_\tau = 10^5$, there is hardly any visible difference between U^+/U^+_{as} and unity anymore. There is also hardly any difference between the flows considered. We note that the neglect of boundary effects (the neglect of U^+_3) implies the universal velocity log-law.

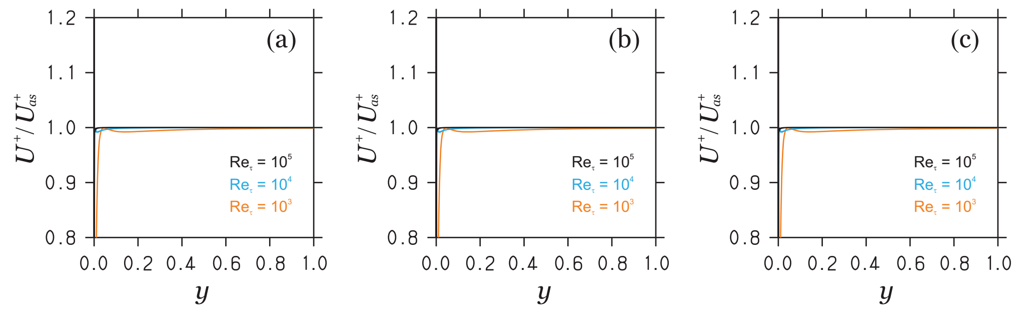

Figure 3. Asymptotic outer velocity scaling of U^+/U^+_{as} with Re_τ along y: (**a**) channel flow, (**b**) pipe flow, (**c**) TBL.

The physical relevance of the asymptotic velocity distribution can be seen by introducing the distribution of mean velocities along the wall-normal direction y,

$$F(U^+_{as}) = \frac{e^{\kappa U^+_{as}} - 1}{e^{\kappa U^+_\infty} - 1} = \frac{e^{\kappa (U^+_{as} - U^+_\infty)} - e^{-\kappa U^+_\infty}}{1 - e^{-\kappa U^+_\infty}} = e^{\kappa (U^+_{as} - U^+_\infty)}. \tag{2}$$

For the flows and range $Re_\tau \geq 500$, the effect of $e^{-\kappa U^+_\infty}$ on $F(U^+_{as})$ is smaller than 0.025%. Thus, the neglect of $e^{-\kappa U^+_\infty}$ is well justified, which explains the last expression in Equation (2). The corresponding PDF $f(U^+_{as}) = dF(U^+_{as})/dU^+_{as}$ reads

$$f(U^+_{as}) = \kappa e^{\kappa (U^+_{as} - U^+_\infty)} = \kappa F(U^+_{as}). \tag{3}$$

The entropy, S_E, related to the PDF, $f(U_{as}^+)$, is defined by $S_E = -\int_0^{U_\infty^+} ln(f) f dU_{as}^+$. Using the definition of $f(U_{as}^+)$ for the entropy, we obtain

$$S_E = 1 - ln\,\kappa - e^{-\kappa U_\infty^+}(1 + \kappa U_\infty^+ + ln\,\kappa) = 1 - ln\,\kappa. \quad (4)$$

The last expression results from the neglect of $e^{-\kappa U_\infty^+}$, as justified above. Hence, the von Kármán constant is an entropy measure, $\kappa = e^{1-S_E}$. It is of interest to compare Equation (2) and Equation (3), which apply to the flow-specific asymptotic velocity distributions with corresponding expressions that neglect the flow dependence. According to Equation (1), we have $U_{as}^+ = \kappa^{-1} ln(y^+) + 5.03$ with $U_\infty^+ = \kappa^{-1} ln(Re_\tau) + 5.03$ in the latter case. By referring to the flow-independent distribution function and PDF as $F_0(U_{as}^+)$ and $f_0(U_{as}^+)$, respectively, we find the expressions

$$F_0(U_{as}^+) = min(y, 1), \qquad f_0(U_{as}^+) = \kappa F_0(U_{as}^+) = \kappa\, min(y, 1). \quad (5)$$

The distribution functions F and F_0 are shown in Figure 4 for the three flows considered. It can be seen that the influence of the flow considered only modifies F_0, obtained by the neglect of boundary effects. The structure of F_0 is the simplest possible interpolation between the limit cases at $F_0(0) = 0$ and $F_0(1) = 1$, respectively.

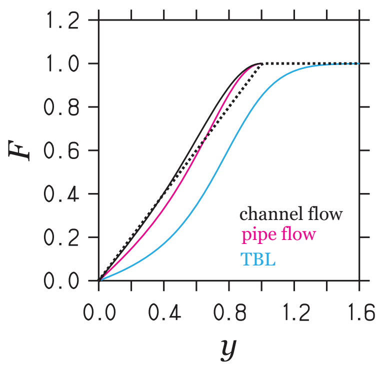

Figure 4. The distribution function F for the distribution of mean velocities along the wall-normal direction y for the three flows considered. The black dashed line shows F_0 obtained by the neglect of boundary effects.

Characteristic properties of turbulence can be well studied by considering characteristic outer-scale velocity, time, and length scales u_∞, τ_∞, and ℓ_∞, respectively, which are defined in Table 2. Instead of directly considering these variables, it is more appropriate to consider the convergence of the Reynolds shear stress $-\langle u'v'\rangle^+$ and turbulence Reynolds number $Re_* = -\langle u'v'\rangle^+/S^+$ based on u_τ. We note that $Re_* = \nu_t^+$ is equivalent to the inner-scale turbulence viscosity. Given converged profiles for $-\langle u'v'\rangle^+$ and Re_*, asymptotic u_*, τ_*, ℓ_* and u_∞, τ_∞, ℓ_∞ can easily be calculated.

Figures 5 and 6 present the convergence properties of $-\langle u'v'\rangle^+$ and $Re_* = -\langle u'v'\rangle^+/S^+$ for the three flows considered. In similarity to the convergence of U^+ to U_{as}^+, it is found that $-\langle u'v'\rangle^+$ and $Re_* = -\langle u'v'\rangle^+/S^+$ approach their asymptotic values for $Re_\tau = 10^5$. The implied asymptotic profiles for the turbulence velocity, time, and length scales based on u_τ are given by

$$u_* = M^{1/2}, \quad \tau_* = \frac{\kappa y^+}{1 + \kappa y^+ S_3^+}, \quad \ell_* = u_* \tau_* = M^{1/2}\tau_*, \quad Re_* = u_* \ell_* = M\tau_*. \quad (6)$$

Using the relationships presented in Table 2, the implied asymptotic profiles of u_∞, τ_∞, and ℓ_∞ are found to be given by the following functions of only y:

$$u_\infty = \frac{M^{1/2}}{U_\infty^+}, \quad \tau_\infty = \frac{\kappa y}{1 + \kappa y^+ S_3^+} U_\infty^+, \quad \ell_\infty = \frac{\kappa y}{1 + \kappa y^+ S_3^+} M^{1/2}, \quad Re_\infty = \frac{\kappa y}{1 + \kappa y^+ S_3^+}\frac{M}{U_\infty^+}. \quad (7)$$

Figure 7 presents the corresponding asymptotic distributions of turbulence velocity scales, time scales, length scales, and turbulence Reynolds numbers for the three flows considered. Independent of specific distributions, the most relevant observation is that the turbulence asymptotically decays, as may be seen from the Re_∞ trends under consideration of the fact that $Re_\infty \sim 1/U_\infty^+ \to 0$, where $U_\infty^+ = 5.03 + \kappa^{-1} ln(Re_\tau/K)$. In correspondence to that, we find that the turbulence velocity scale vanishes, $u_\infty \sim 1/U_\infty^+ \to 0$, and the time scale $\tau_\infty \sim U_\infty^+ \to \infty$. The structure of $Re_\infty U_\infty^+ = Re_*/Re_\tau$ corresponds to the expectations: for channel and pipe flow, we see damping-function-type distributions along y that approache a constant Reynolds number at the centerline. For the TBL, the flow becomes laminar under freestream conditions.

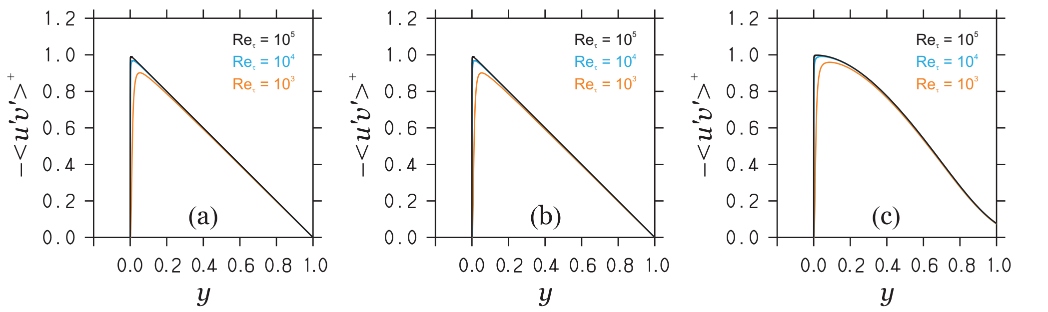

Figure 5. Asymptotic outer Reynolds shear stress scaling with Re_τ along y: (**a**) channel flow, (**b**) pipe flow, (**c**) TBL.

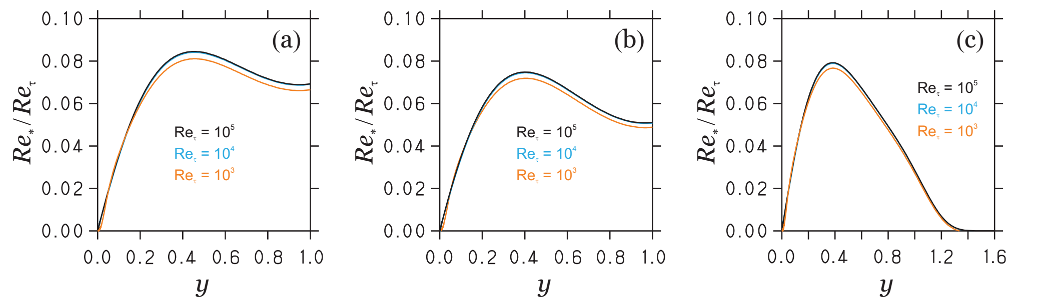

Figure 6. Asymptotic outer turbulence Re_* scaling with Re_τ along y: (**a**) channel flow, (**b**) pipe flow, (**c**) TBL. The difference between $Re_\tau = 10^4$ and $Re_\tau = 10^5$ is hardly visible.

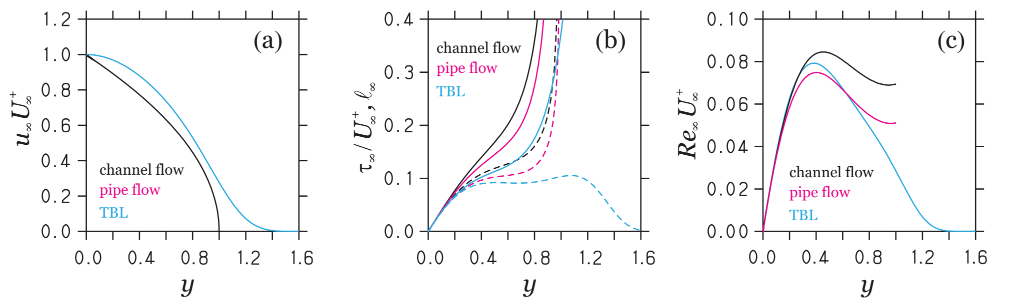

Figure 7. Asymptotic outer scaling for the three flows considered: (**a**) turbulence velocity scale $u_* = u_\infty U_\infty^+$ [there is no visible difference between black and magenta curves], (**b**) turbulence time $\tau_*/Re_\tau = \tau_\infty/U_\infty^+$ and length scales $\ell_*/Re_\tau = \ell_\infty$ (dashed lines), and (**c**) $Re_*/Re_\tau = Re_\infty U_\infty^+$.

The distribution of the length scale ℓ_∞ seen in Figure 7 is of particular interest. In contrast to the other variables (Re_∞, u_∞, and τ_∞), ℓ_∞ is finite over most of the domain. In particular, near the wall, ℓ_∞ follows $\ell_\infty = \kappa y$ according to Equation (7) for all the flows considered. The latter provides strong support for the suitability of Prandtl's debated mixing length concept [35–41]. For channel and pipe flow, ℓ_∞ diverges for $y \to 1$, and the size of turbulence structures can become unbounded. For the TBL case we see that ℓ_∞

approaches zero under freestream conditions, which is consistent with the Re_∞ behavior showing flow laminarization. An interesting observation is that $f_0(U_{as}^+) = \kappa y$ is equivalent to the outer turbulence length scale $\ell_\infty = \kappa y$ for $0 \leq y \leq 1$, which shows a mean flow—turbulence balance.

4. Inner Scaling Implications

In regard to the inner scaling y^+ variations, there are no wake contributions S_3^+ such that $S^+ = S_1^+ + S_2^+$, and the momentum balance $S^+ - \langle u'v' \rangle^+ = M$ reduces to $-\langle u'v' \rangle^+ = 1 - S_1^+ - S_2^+$. Using the abbreviation $S_{12}^+ = S_1^+ + S_2^+$, the inner-scale characteristic turbulence velocity, time, and length scales and Re_* read

$$u_* = \sqrt{1 - S_{12}^+}, \quad \tau_* = 1/S_{12}^+, \quad \ell_* = u_* \tau_* = \sqrt{1 - S_{12}^+}/S_{12}^+, \quad Re_* = u_* \ell_* = (1 - S_{12}^+)/S_{12}^+. \tag{8}$$

Using the definition of Re_*, the latter relations can be also written as

$$u_* = \sqrt{1 - 1/(1 + Re_*)}, \quad \tau_* = 1 + Re_*, \quad \ell_* = Re_* \sqrt{1 + 1/Re_*}. \tag{9}$$

The corresponding outer-scale variables are then given by

$$u_\infty = \frac{u_*}{U_\infty^+}, \quad \tau_\infty = \frac{\tau_* U_\infty^+}{Re_\tau}, \quad \ell_\infty = \frac{\ell_*}{Re_\tau}, \quad Re_\infty = \frac{Re_*}{Re_\tau U_\infty^+}. \tag{10}$$

The asymptotic distributions of the velocity and turbulence characteristics are illustrated in Figure 8. Figure 8a shows that the convergence of U^+ to U_{as}^+ with increasing Re_τ is clearly a characteristic feature of outer scaling: there is no such convergence with respect to inner scaling. This figure also shows the difference between $U_1^+/U_{1\infty}^+$ and $U_2^+/U_{1\infty}^+$ contributions: the effect of $U_2^+/U_{1\infty}^+$ is rather little for the y^+ range considered. There is a remarkable agreement between the variations in $U_1^+/U_{1\infty}^+$ and u_*. Both $U_1^+/U_{1\infty}^+$ and u_* are driven by the damping of the Reynolds shear stress due to the presence of the wall.

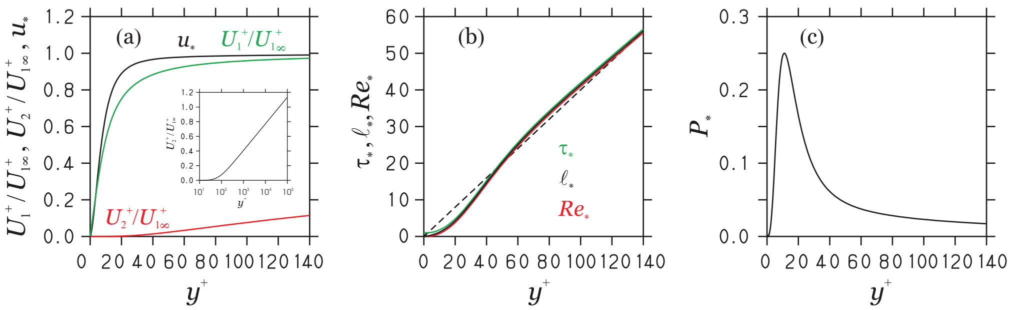

Figure 8. Asymptotic inner scaling along y^+: (**a**) $U_1^+/U_{1\infty}^+$ and $U_2^+/U_{1\infty}^+$, where $U_{1\infty}^+ = 15.85$ and u_*; (**b**) ℓ_*, τ_*, and Re_*; and (**c**) $P_* = (1 - 1/\tau_*)/\tau_*$. The inset in (**a**) shows the variation in $U_2^+/U_{1\infty}^+$ for a much larger range of y^+. The dashed lines in (**b**) shows κy^+.

Figure 8b shows the near-wall variations in ℓ_*, τ_*, and Re_*. In agreement with Equation (9), we see only minor differences between ℓ_*, τ_*, and Re_*. For a sufficiently large Re_*, we have $\ell_* = \tau_* = Re_*$. Because of $\tau_* = \kappa y^+/(\kappa y^+ S_{12}^+)$ being combined with the asymptotic $\kappa y^+ S_{12}^+ = 1$, the values of ℓ_*, τ_*, and Re_* asymptotically approach κy^+, as may be seen in Figure 8b. The latter is consistent with the corresponding transition into outer scaling variations given in Figure 7. The implications for the outer-scale variables given in Equation (10) are consistent with the corresponding implications of outer scaling: u_∞ and Re_∞ asymptotically vanish, and τ_∞ goes to infinity. On the other hand, we find $\ell_\infty = \kappa y$, i.e., finite ℓ_∞ variations, controlled by the distance to the wall.

Figure 8c shows the asymptotic distribution of the production of kinetic energy, $P_* = (1 - 1/\tau_*)/\tau_*$. The analysis of P_* variations shows that P_* has a maximum of $P_* = 1/4$ at $\tau_* = 2$ corresponding to $y^+ = 11.0694$. Thus, turbulence is still present in inner scaling at infinite Re_τ, although the turbulence decays in outer scaling.

5. Summary

The asymptotic structure of wall-bounded turbulent flows is reported here for the first time for three canonical flows independent of a modeling assumption in conflict with the universality of the law of the wall and other modeling assumptions with uncertain support. The results obtained can be summarized as follows.

In regard to outer scaling considered to be function of y, there is a trend that the mean velocity U^+ approaches the constant U^+_∞. However, this convergence is so slow that there are clear differences between U^+ and U^+_∞, even for $Re_\tau = 10^{120}$. It has to be expected, therefore, that U^+ is still different from U^+_∞ under conditions of practical relevance. On the other hand, U^+ converges to U^+_{as} for about $Re_\tau = 10^5$. It is beneficial to discuss this asymptotic velocity distribution in terms of the implied PDF of the distribution of mean velocities along the wall-normal direction y. In absence of boundary conditions (in absence of wake contributions), a linear mean velocity PDF was found to be equivalent to the length scale distribution of turbulence. The wake effect adjusts the PDF to the boundary conditions. Considered again in outer scaling, asymptotic outer-scale turbulence characteristic velocity, time, and length scales observed for about $Re_\tau = 10^5$ reveal features in consistency with the mean velocity trend toward a spatial smoothing. The turbulence decays: Re_∞ and u_∞ approach zero. Simultaneously, the turbulence time scale τ_∞ approaches infinity, which indicates frozen turbulence structures. In contrast to the other variables, it is of interest to note that the turbulence length scale ℓ_∞ is finite throughout the domain except at the centerline for channel and pipe flows. The latter provides strong support for the suitability of Prandtl's debated mixing length concept [35]. In particular, not too far from the wall ℓ_∞ is proportional to the distance y from the wall with the von Kármán constant κ as a proportionality constant.

For infinite Re_τ, inner scaling reveals flow features in an infinitesimally thin layer close to the wall. Inner scaling features (considered as function of y^+) of the variables considered are the following ones. The mean velocity U^+ is finite and characterized by the damping effect of the wall. The behavior of the main component $U^+_1/U^+_{1\infty}$ in this region is very similar to the corresponding behavior of the turbulence velocity u_*. The correlation between $U^+_1/U^+_{1\infty}$ and u_* can be explained by the wall-damping effect on the Reynolds shear stress. Turbulence survives in this infinitesimally thin layer close to the wall, as can be seen from the distribution of production P_* and the u_* distribution. The characteristic time and length scales τ_* and ℓ_* show trends in consistency with their outer scaling trends: τ_* approaches infinity and ℓ_* approaches κy^+ (corresponding to $\ell_\infty = \kappa y$).

The results reported here are very beneficial in regard to several questions.

1. DNS and experimental studies are supposed to provide essential contributions to the validation of simpler computational methods. Unfortunately, such studies suffer significantly from the uncertainty of their predictions for high Re_τ [6–8,12]. The results reported here are, therefore, essential to understand the requirements for accurate DNS and experimental studies.
2. One of the basic problems of turbulence modeling is the uncertainty of the scale (ϵ or ω) equation: existing equations are considered to have a rather weak theoretical basis. Similar to recent work [21], the distributions of turbulence variables determined here can be used for the validation or improvements of scale equations.
3. The existence and structure of asymptotically stable turbulence regimes is debated in regard to many turbulent flows (e.g., for complex hump-type flows involving flow separation [19,20]). The identification of asymptotic Re_τ regimes as reported here matters to such discussions. The latter provides insight into Re_τ values needed to observe asymptotic regimes, and insight of which mean velocity and turbulence structures enable asymptotically stable turbulent flows.

Funding: I would like to acknowledge support from the National Science Foundation (AGS, Grant No. 2137351, with N. Anderson as Technical Officer) and support from the Hanse-Wissenschaftskolleg (Delmenhorst, Germany, with M. Kastner as Technical Officer). This work was supported by Wyoming NASA Space Grant Consortium (NASA Grant No. 80NSSC20M0113).

Data Availability Statement: Data are contained within the article.

Conflicts of Interest: The author declares no conflict of interests.

References

1. von Kármán, T. Mechanische Ähnlichkeit und Turbulenz [Mechanical similitude and turbulence]. In *Nachrichten der Akademie der Wissenschaften Göttingen, Mathematisch-Physikalische Klasse*; Technical Memorandum N611; National Advisory Committee for Aeronautics: Washington, DC, USA, 1931; pp. 58–76.
2. Marusic, I.; McKeon, B.J.; Monkewitz, P.A.; Nagib, H.M.; Smits, A.J.; Sreenivasan, K.R. Wall-bounded turbulent flows at high Reynolds numbers: Recent advances and key issues. *Phys. Fluids* **2010**, *22*, 65103. [CrossRef]
3. Smits, A.J.; McKeon, B.J.; Marusic, I. High-Reynolds number wall turbulence. *Annu. Rev. Fluid Mech.* **2011**, *43*, 353–375. [CrossRef]
4. Jiménez, J. Near-wall turbulence. *Phys. Fluids* **2013**, *25*, 101302. [CrossRef]
5. Luchini, P. Universality of the turbulent velocity profile. *Phys. Rev. Lett.* **2017**, *118*, 224501. [CrossRef]
6. Heinz, S. On mean flow universality of turbulent wall flows. I. High Reynolds number flow analysis. *J. Turbul.* **2018**, *19*, 929–958. [CrossRef]
7. Heinz, S. On mean flow universality of turbulent wall flows. II. Asymptotic flow analysis. *J. Turbul.* **2019**, *20*, 174–193. [CrossRef]
8. Cantwell, B.J. A universal velocity profile for smooth wall pipe flow. *J. Fluid Mech.* **2019**, *878*, 834–874. [CrossRef]
9. Subrahmanyam, M.A.; Cantwell, B.J.; Alonso, J.J. A universal velocity profile for turbulent wall flows including adverse pressure gradient boundary layers. *J. Fluid Mech.* **2022**, *933*, A16. [CrossRef]
10. Monkewitz, P.A. Revisiting the quest for a universal log-law and the role of pressure gradient in "canonical" wall-bounded turbulent flows. *Phys. Rev. Fluids* **2017**, *2*, 94602. [CrossRef]
11. Monkewitz, P.A. The late start of the mean velocity overlap log law at–a generic feature of turbulent wall layers in ducts. *J. Fluid Mech.* **2021**, *910*, A45. [CrossRef]
12. Monkewitz, P.A.; Nagib, H.M. The hunt for the Kármán 'constant' revisited. *J. Fluid Mech.* **2023**, *967*, A15. [CrossRef]
13. Pirozzoli, S.; Smits, A.J. Outer-layer universality of the mean velocity profile in turbulent wall-bounded flows. *Phys. Rev. Fluids* **2023**, *8*, 64607. [CrossRef]
14. Chen, X.; Sreenivasan, K.R. Reynolds number asymptotics of wall-turbulence fluctuations. *J. Fluid Mech.* **2023**, *976*, A21. [CrossRef]
15. Pope, S.B. *Turbulent Flows*; Cambridge University Press: Cambridge, UK, 2000.
16. Heinz, S. From Two-Equation Turbulence Models to Minimal Error Resolving Simulation Methods for Complex Turbulent Flows. *Fluids* **2022**, *7*, 368. [CrossRef]
17. Heinz, S. Minimal error partially resolving simulation methods for turbulent flows: A dynamic machine learning approach. *Phys. Fluids* **2022**, *34*, 51705. [CrossRef]
18. Heinz, S. The Continuous Eddy Simulation Capability of Velocity and Scalar Probability Density Function Equations for Turbulent Flows. *Phys. Fluids* **2021**, *33*, 25107. [CrossRef]
19. Heinz, S. A review of hybrid RANS-LES methods for turbulent flows: Concepts and applications. *Prog. Aerosp. Sci.* **2020**, *114*, 100597. [CrossRef]
20. Heinz, S.; Mokhtarpoor, R.; Stoellinger, M.K. Theory-Based Reynolds-Averaged Navier-Stokes Equations with Large Eddy Simulation Capability for Separated Turbulent Flow Simulations. *Phys. Fluids* **2020**, *32*, 65102. [CrossRef]
21. Plaut, E.; Heinz, S. Exact eddy-viscosity equation for turbulent wall flows—Implications for computational fluid dynamics models. *AIAA J.* **2022**, *60*, 1347–1364. [CrossRef]
22. Heinz, S.; Heinz, J.; Brant, J.A. Mass Transport in Membrane Systems: Flow Regime Identification by Fourier Analysis. *Fluids* **2022**, *7*, 369. [CrossRef]
23. Kollmann, W. Asymptotic properties of mixing length closures for turbulent pipe flow. *Phys. Fluids* **2020**, *32*, 115126. [CrossRef]
24. Pullin, D.I.; Inoue, M.; Saito, N. On the asymptotic state of high Reynolds number, smooth-wall turbulent flows. *Phys. Fluids* **2013**, *25*, 15116. [CrossRef]
25. Abramowitz, M.; Stegun, I.A. *Pocketbook of Mathematical Functions–Abridged Edition of Handbook of Mathematical Functions*; JSTOR: New York, NY, USA, 1988.

26. Lee, M.; Moser, R.D. Direct numerical simulation of turbulent channel flow up to $Re_\tau = 5200$. *J. Fluid Mech.* **2015**, *774*, 395–415. [CrossRef]
27. 2016. Available online: http://turbulence.ices.utexas.edu (accessed on 1 January 2016).
28. Chin, C.; Monty, J.P.; Ooi, A. Reynolds number effects in DNS of pipe flow and comparison with channels and boundary layers. *Internat. J. Heat Fluid Flow* **2014**, *45*, 33–40. [CrossRef]
29. Sillero, J.A.; Jiménez, J.; Moser, R.D. One-point statistics for turbulent wall-bounded flows at Reynolds numbers up to $\delta^+ \approx 2000$. *Phys. Fluids* **2013**, *25*, 105102. [CrossRef]
30. 2016. Available online: http://torroja.dmt.upm.es/turbdata/blayers (accessed on 1 January 2016).
31. Schultz, M.P.; Flack, K.A. Reynolds-number scaling of turbulent channel flow. *Phys. Fluids* **2013**, *25*, 25104. [CrossRef]
32. Hultmark, M.; Vallikivi, M.; Bailey, S.C.C.; Smits, A.J. Logarithmic scaling of turbulence in smooth-and rough-wall pipe flow. *J. Fluid Mech.* **2013**, *728*, 376–395. [CrossRef]
33. 2016. Available online: https://smits.princeton.edu/superpipe-turbulence-data (accessed on 1 January 2016).
34. Vallikivi, M.; Hultmark, M.; Smits, A.J. Turbulent boundary layer statistics at very high Reynolds number. *J. Fluid Mech.* **2015**, *779*, 371–389. [CrossRef]
35. Prandtl, L. Bericht über die Entstehung von Turbulenz. *Z. Angew. Math. Mech.* **1925**, *5*, 136–139. [CrossRef]
36. Bradshaw, P. Possible origin of Prandt's mixing-length theory. *Nature* **1974**, *249*, 135–136. [CrossRef]
37. Egolf, P.W. Difference-quotient turbulence model: A generalization of Prandtl's mixing-length theory. *Phys. Rev. E* **1994**, *49*, 1260. [CrossRef] [PubMed]
38. Bodenschatz, E.; Eckert, M. Prandtl and the Göttingen school. In *A Voyage Through Turbulence*; Davidson, P.A., Kaneda, Y., Moffatt, K., Sreenivasan, K.R., Eds.; Cambridge University Press: Cambridge, UK, 2011; pp. 40–100.
39. Örlü, R.; Fransson, J.H.M.; Alfredsson, P.H. On near wall measurements of wall bounded flows—The necessity of an accurate determination of the wall position. *Prog. Aerosp. Sci.* **2010**, *46*, 353–387. [CrossRef]
40. Baumert, H.Z. Universal equations and constants of turbulent motion. *Phys. Scr.* **2013**, *2013*, 14001. [CrossRef]
41. Ali, S.Z.; Dey, S. The law of the wall: A new perspective. *Phys. Fluids* **2020**, *32*, 121401. [CrossRef]